Available online at www.sciencedirect.com
ScienceDirect
Proceedings of the Combustion Institute 000 (2018) 1–8
Proceedings of the Combustion Institute
www.elsevier.com/locate/proci

# Effects of combustion models on soot formation and evolution in turbulent nonpremixed flames

Wang Han [a,b,*,**], Venkat Raman [a], Michael E. Mueller [c], Zheng Chen [b]

[a] Department of Aerospace Engineering, The University of Michigan, Ann Arbor, MI 48109, USA
[b] SKLTCS, Department of Mechanics and Engineering Science, Peking University, Beijing 100871, China
[c] Department of Mechanical and Aerospace Engineering, Princeton University, Princeton, NJ 08544, USA

Received 30 November 2017; accepted 13 June 2018
Available online xxx

**Abstract**

Due to the complex multiscale turbulence–chemistry-soot (TCS) interactions in sooting flames, developing predictive models remains a formidable challenge even with the improved accuracy of the large eddy simulation (LES) approach. LES-based soot models have three main components: a) models for gas-phase chemistry and precursor evolution, b) models for soot particle dynamics, and c) models for subfilter scale TCS interactions. The focus of this work is this latter aspect, for several recent studies have shown that subfilter correlations between the gas-phase and the soot particles are of primary importance in affecting predictability. To this end, a consistent LES/probability density function (PDF) approach with detailed chemistry (denoted as full transport and chemistry (FTC)) and state-of-the-art soot models is used to accurately characterize subfilter TCS interactions. The statistical soot model is based on the Hybrid Method of Moments (HMOM), considering detailed nucleation, condensation, coagulation, surface growth, oxidation, and fragmentation processes. To study the sensitivity of soot predictions to combustion model, tabulated chemistry based on the radiation flamelet/progress variable (RFPV) approach is accounted for in the LES/PDF framework. The Delft-Adelaide natural gas jet flame is simulated to investigate the effects of combustion models on soot predictions. It is found that the location of inception and soot evolution are rather sensitive to the combustion model. Compared to the PDF/RFPV model, the PDF/FTC model improves the simulation results and predicts lower soot volume fraction with soot formation and growth further downstream. Accounting for detailed subfilter TCS interactions through the PDF/FTC model suppresses the contributions of aromatic-based soot growth (nucleation and condensation), while the contribution of acetylene-based surface growth is significantly enhanced and even dominates over condensation at downstream locations. These results imply that the choice of combustion model has a significant impact on the characterization of subfilter TCS interactions due to the strong coupling between turbulence, soot, and chemistry. The tabulated chemistry

* Corresponding author at: Department of Aerospace Engineering, The University of Michigan, Ann Arbor, MI 48109, USA.
** Current address: STFS, TU Darmstadt, Germany.
*E-mail addresses:* han@stfs.tu-darmstadt.de, whan@pku.edu.cn (W. Han).

https://doi.org/10.1016/j.proci.2018.06.096

approach probably cannot capture the high sensitivity of soot formation and growth phases to the history of turbulent gas-phase compositions encountered.


*Keywords:* Turbulence-chemistry-soot interactions; LES/PDF approach; Detailed chemistry; HMOM

## 1. Introduction

Computational modeling of soot formation in turbulent flames has remained a formidable challenge due to the high sensitivity of soot particle evolution to the history of gas-phase compositions encountered. Previous studies have shown that soot formation is spatially intermittent [1,2], which could be attributed to multiple causes. In jet-like flames, such intermittency is predominantly driven by the sensitivity of soot precursor evolution to local strain rates [3]. In more complex flows with strong recirculation regions, the slow time-scales within these regions combined with the large-scale unsteadiness can lead to intermittent soot generation [4]. Since soot formation is promoted only by a very narrow range of gas-phase compositions, the ability to accurately describe the interaction of the turbulent gas-phase with particle motion becomes critical. In particular, the ability to model the effect of time-correlated turbulent fluctuations of the gas-phase is important [3,5].

Here, the modeling framework will be based on the large eddy simulation (LES) approach. Over the last decade, the use of LES has gained prominence due to its ability to describe large scale mixing accurately. However, small-scale processes require detailed modeling. While macroscopic properties related to the gas-phase are relatively insensitive to small-scale models for flames that are far from extinction, soot formation and other small-scale driven phenomena require extensive modeling. In the LES context, detailed description of soot formation involves three main components: a) models for gas-phase chemistry and precursor evolution, b) models for soot particle dynamics, and c) models for subfilter scale turbulence–chemistry-soot (TCS) interactions [6,7]. While modeling of the first two components is equivalent to that in laminar flames [8,9], the LES-based description of subfilter TCS interactions faces unique challenges [7].

The LES approach requires closures for small-scale correlations, which can be cast as models for a suitably defined one-point one-time probability density function (PDF) [10–12]. The gas-phase thermochemical state is expressed in terms of the composition vector $\boldsymbol{\phi}$, while the soot particle population is evolved using a finite-set of moments $\boldsymbol{\mathcal{M}}$, which can be used to approximately reconstruct the number density function [13–15]. The one-point one-time PDF then describes the joint probability of the extended species vector $\boldsymbol{\psi} = \{\boldsymbol{\phi}, \boldsymbol{\mathcal{M}}\}$. There are many approaches to modeling this joint-PDF. In the presumed PDF methods [16–18], the joint-PDF is assumed to be statistically independent and hence can be written as the product of marginal PDFs of $\boldsymbol{\phi}$ and $\boldsymbol{\mathcal{M}}$, which removes all small-scale correlations between soot and the gas-phase, but retains the filter-level correlations due to the LES formulation. It is expected that the assumption could potentially be violated in the soot growth and oxidation phases because of the strong interactions between soot and gas-phase in these processes.

The most comprehensive approach is to solve the joint-PDF of $\boldsymbol{\psi}$ directly with the transported PDF approach [19]. While this approach has been successfully applied to a variety of gas-phase flames [11,20–23], there are only a few studies on the application of the approach to sooting flames [12,24–26]. In the RANS modeling framework, Zamuner and Dupoirieux [24] studied the effects of turbulent fluctuations on soot formation with a skeletal soot model. Mehta et al. [25] investigated the effects of radiation losses on luminous turbulent jet flames by coupling the PDF method to a photon Monte Carlo method. Lindstedt and Louloudi [26] found that a comparatively simple soot model also has the potential to provide good soot predictions when combined with the transported PDF approach. They highlighted the importance of accurate modeling of turbulence–chemistry interactions. In the context of LES-based simulation of turbulent sooting flames, this approach has been used with a semi-empirical sooting model albeit with simplified chemical kinetics [27]. To accurately capture soot inception and the formation of soot precursors such as acetylene and PAH, a detailed chemical mechanism accounting for all major pathways of PAH formation is needed, and may involve hundreds of species and thousands of reactions [28,29]. Typically, the flamelet-based combustion models combined with the presumed PDF model [4,16–18] are used to reduce the computational cost. However, their suitability for the description of detailed soot–chemistry interactions has not been fully explored. On the other hand, the transported PDF model offers a potential to incorporate the state-of-the-art soot models based on the detailed mechanism without any assumption about the flame topology structure, and meanwhile provides the joint-PDF without simplifications.

Please cite this article as: W. Han et al., Effects of combustion models on soot formation and evolution in turbulent nonpremixed flames, Proceedings of the Combustion Institute (2018), https://doi.org/10.1016/j.proci.2018.06.096

However, the computational cost is higher due to direct treatment of chemical kinetics.

With this background, the objective of this work is threefold: (1) to accurately characterize detailed small-scale TCS interactions using a consistent LES/PDF approach with detailed gas-phase chemistry and state-of-the-art soot models; (2) to study the sensitivity of soot predictions to the choice of combustion model by accounting for two different combustion models, namely detailed chemistry and flamelet-based tabulated chemistry; and (3) to investigate the effects of combustion models on the characterization of subfilter TCS interactions.

## 2. Modeling framework

### 2.1. Soot model

The soot particle evolution is described by a population balance equation (PBE) [6,13], which tracks the evolution of the number density function (NDF) $N(\boldsymbol{\xi}; \boldsymbol{x}, t)$ where each particle type is characterized by an internal coordinate vector \boldmath $\xi$. In order to describe the fractal aggregates of soot particles, volume $V$ and surface area $S$ are used to characterize the NDF. The hybrid method of moments (HMOM [7]) is used, where four lower-order moments of the NDF are solved. The moment source terms involve complex physical and chemical processes that drive the formation and evolution of soot particles due to nucleation, condensation, coagulation, surface growth, and oxidation [7]. PAH-based nucleation and condensation are employed in this work, and surface growth is described by the H-abstraction-$C_2H_2$-addition (HACA) mechanism [30]. Details regarding the modeling of these processes can be found in Mueller et al. [7] and the references therein. As discussed below, these moments are integrated with the gas-phase composition field using a PDF approach.

### 2.2. Subfilter turbulence–chemistry-soot interactions

Unlike the presumed PDF method that assumes the $\boldsymbol{\phi}$ and $\boldsymbol{\mathcal{M}}$ to be statistically independent, here the one-point, one-time density-weighted joint-PDF of $\boldsymbol{\psi}, f(\boldsymbol{\varphi}; \boldsymbol{x}, t)$, is directly evolved with the following expression to accurately describe the TCS interactions.

$$\frac{\partial f}{\partial t} + \nabla \cdot (\widetilde{\boldsymbol{u}} f) = \nabla \cdot [\overline{\rho} D_t \nabla (f/\overline{\rho})] - \frac{\partial}{\partial \psi_\alpha}\left[\left(\frac{1}{\overline{\rho}}\overline{\nabla \cdot (\rho D_\alpha \nabla \psi_\alpha)|\boldsymbol{\varphi}} + S_\alpha(\boldsymbol{\varphi})\right) f\right] \tag{1}$$

where $\boldsymbol{\varphi}$ denotes the composition sample space of $\boldsymbol{\phi}$. $D_t$ is the eddy diffusivity, $\overline{\nabla \cdot (\rho D_\alpha \nabla \psi_\alpha)|\boldsymbol{\varphi}}$ the conditional micromixing term that is described by the IEM model [31], $S_\alpha$ the chemical reaction/moment source terms for thermochemical composition/moment component $\alpha$, and $D_\alpha$ the corresponding molecular diffusivity of the component. The new framework of the self-conditioned PDF [32] is used here. In this context, the LES mean density is $\overline{\rho} = 1/\int f/\rho(\boldsymbol{\varphi}) d\boldsymbol{\varphi}$, and the LES mean composition $\widetilde{\boldsymbol{\psi}} = (\widetilde{\boldsymbol{\phi}}, \overline{\mathcal{M}})$ can be obtained by taking the first moment of the PDF: $\widetilde{\boldsymbol{\psi}} = \int \boldsymbol{\varphi} f d\boldsymbol{\varphi}$. It is noted that the overline "–" denotes the filtering operation in the traditional filtering viewpoint in LES/PDF [23,33]. Practically, both viewpoints of LES/PDF do not lead to substantially different partial differential equations to be solved.

### 2.3. Combustion model

To investigate the sensitivity of soot predictions to the combustion process, two different combustion models for describing gas-phase and soot chemistry are considered: (1) detailed chemistry denoted as full transport and chemistry (FTC); and (2) tabulated chemistry based on the radiation flamelet/progress variable (RFPV) approach [16]. In the FTC model, the composition is represented by the full thermochemical state variables, i.e., $\boldsymbol{\phi} = [Y_1, \ldots, Y_N, h]^T$, where $N$ is the number of species in the chemical mechanism. The soot-related quantities $\boldsymbol{\phi}^s$ (e.g., surface reaction rate coefficient, oxidation rate coefficient, fragmentation rate coefficient, and soot formation related quantities) are directly calculated using the full thermochemical state. It is expected that the PDF/FTC model can capture comprehensive soot-chemistry interactions. On the other hand, in the RFPV model the thermochemical state $\boldsymbol{\phi}$ and soot-related quantities $\boldsymbol{\phi}^s$ are mapped into mixture fraction $Z$ and progress variable $C$ space by a series of flamelet solutions ; A third coordinate $H$ is included in the mapping process to account for radiation losses by solving the unsteady flamelet equations. The complete mapping that provides any gas-phase composition and soot-related quantities can be written as $\boldsymbol{\phi} = \boldsymbol{\phi}(Z, C, H)$ and $\boldsymbol{\phi}^s = \boldsymbol{\phi}^s(Z, C, H)$. An additional transport equation for the total mass fraction $Y_{\mathrm{PAH}}$ is solved to describe the unsteady evolution of PAH concentration. In the RFPV model context, the complete set $\boldsymbol{\psi} = (\boldsymbol{\phi}, \boldsymbol{\mathcal{M}})$ is replaced with the reduced set $\boldsymbol{\psi} = (Z, C, H, Y_{\mathrm{PAH}}, \boldsymbol{\mathcal{M}})$. Here, the chemical mechanism [16,29] accounting for all major pathways of PAH formation is used in the above two combustion models. The detailed mechanism has been extensively validated for soot formation and evolution in different flame configurations [4,7,16,18]. It is noted that the uncertainties in the PAH chemistry have a significant impact on soot prediction. These effects deserve further investigation in future work.

Please cite this article as: W. Han et al., Effects of combustion models on soot formation and evolution in turbulent nonpremixed flames, Proceedings of the Combustion Institute (2018), https://doi.org/10.1016/j.proci.2018.06.096

## 3. Numerical implementation

The LES/PDF approach for sooting flames involves two different solvers that are time-accurately coupled: a) a low-Mach number LES solver that evolves gas-phase density, velocity and energy fields, and b) a transported-PDF solver that advances the gas composition and soot moments in time and space. The coupling between LES and PDF solvers has been studied extensively studied [20,21,33,34]. Here, a Lagrangian Monte-Carlo (MC) approach is used to evolve the transported PDF equation [19]. Details of the PDF solver are provided in [12,20].

In order to extend the PDF approach to turbulent sooting flames, three issues have to be considered. First, the micro-mixing of the soot moments is neglected due to high Schmidt number of soot particle, which implies the mixing frequency of soot moments is close to zero. This takes into account a preferential transport between soot and the gas-phase at small-scales. The mixing time-scale of gas-phase composition is determined through a dynamic procedure [11,20], which removes the need to specify the value of model constant. In this work, the unity Lewis number assumption is used in both RFPV and FTC models. Second, incorporating detailed chemical kinetics is computationally expensive. This is further complicated by the presence of stiff kinetics associated with soot moment evolution. In this work, the ISAT algorithm [35] is employed in the FTC model to accelerate the chemistry integration of each MC particle in composition space. In order to achieve load balance and parallel scale-up, the MC particles are grouped based on mixture fraction and distributed among processors. Each processor thus builds a tree that is nearly local in composition space, thereby reducing the ISAT tabulations further. This grouping and re-distribution procedures are updated at each time-step. A scale-up of 5–10 times is obtained compared to building ISAT tables independently on each processor. To account for heat loss effect on soot formation in the FTC model, flame radiation is considered and modeled using the RADCAL model [36]. Soot radiation is neglected due to the small soot volume fraction in the validation flame. Thermophoresis of soot particles was found to be negligible [12] and, therefore, is not included here. Third, it is challenging to couple the low Mach number LES solver with the PDF solver because the gas-phase density directly obtained from the PDF solver contains statistical noise due to the finite number of particles per filter volume, which can cause numerical instabilities. To address this issue, the transported specific volume (TSV) approach [37] is used in the present work, where an additional scalar, specific volume, is transported in the LES solver to obtain the gas-phase density.

## 4. Delft-Adelaide flame: simulation details

The Delft-Adelaide flame [1,38], which is one of the target flames for the International Sooting Flames (ISF) workshop, is used to study the impact of TCS modeling on LES predictions. The burner consists of a fuel jet with a diameter of $D = 6$ mm, through which natural gas at a temperature of 300 K and exit bulk velocity of $U = 21.9$ m/s is supplied. The jet is surrounded by an annulus of primary air stream with inner/outer diameters of 15 mm and 45 mm, respectively. The air stream velocity is 4.4 m/s. The turbulent nonpremixed jet flame is stabilized by twelve small pilot flames that are arranged in a ring between the fuel jet and the air annulus. The burner is placed in a slow air colfow with the velocity of 0.3 m/s. Detailed species profiles are available at upstream locations, while soot volume fraction measurements are available for downstream locations.

The LES/PDF/FTC and LES/PDF/RFPV calculations are performed using a cylindrical coordinate system $(x,\ r,\ \theta)$ with a computational domain of $L_x \times L_r \times L_\theta = 150D \times 43D \times 2\pi$ in the axial, radial and azimuthal directions, respectively. A non-uniform stretched grid of size $N_x \times N_r \times N_\theta = 384 \times 192 \times 64$ is used to resolve the central jet and the shear layers. The turbulent jet boundary conditions for fuel jet and primary air stream are obtained from a separate simulation of the burner geometry. The bulk inflow boundary is used for the coflow air. The jet reaches the statistically stationary state at $t/T_j \approx 10$, where $T_j$ is the flow-through time. Statistics are collected over 8 flow-through times. All simulations are conducted in parallel using domain decomposition along with ISAT redistribution (discussed above), using 288 processors. The two closures require 8 and 163 state variables, and cost about 0.07 and 1.05 million CPU hours, respectively. The LES/PDF/RFPV approach is about 15 times faster than the LES/PDF/FTC approach when the flame reaches the statistically stationary state.

## 5. Results and discussion

### 5.1. Instantaneous soot evolution

Figure 1 shows the instantaneous fields of temperature, PAH mass fraction, soot volume fraction, and soot number density from the LES/PDF/FTC simulation. It is seen that the formation of PAH and soot is mainly confined to the fuel-rich region inside the stoichiometric surface. While high PAH concentrations increase soot nucleation upstream ($x/D \approx 15$), observable soot volume fraction only occurs after $x/D \approx 50$. From $x/D \approx 60$ to $x/D \approx 100$, soot number density does not change very much while soot volume fraction is significantly in-

Please cite this article as: W. Han et al., Effects of combustion models on soot formation and evolution in turbulent nonpremixed flames, Proceedings of the Combustion Institute (2018), https://doi.org/10.1016/j.proci.2018.06.096

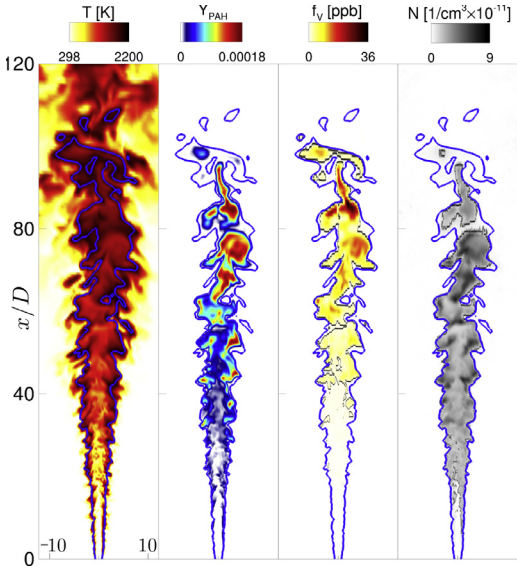


Fig. 1. Representative snapshots (same instant in time) in a cut of the 3D domain of temperature, PAH mass fraction, soot volume fraction and number density from LES/PDF/FTC. The isolines correspond to the stoichiometric mixture fraction $Z_{st} = 0.073$.

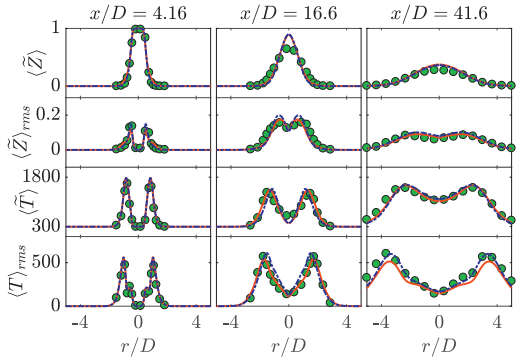


Fig. 2. Time-averaged means and RMS fluctuations of mixture fraction and temperature at three different axial locations. Experiment data (●); LES/PDF/RFPV (- - -) and LES/PDF/FTC (——).

creased, which indicates particle coagulation, PAH condensation, and HACA-based soot growth are dominant in that region. After $x/D \approx 100$, oxidation process proceeds fast to remove most of the soot particles.

### 5.2. Sensitivity to the combustion model

The LES results are first compared to the existing experimental data at upstream locations where measurements are available. Figure 2 shows time-averaged mean and RMS profiles of mixture fraction and temperature. Compared to the PDF/FTC model, the PDF/RFPV model slightly overpredicts the RMS fluctuation of mixture fraction at $x/D =$ 16.6 and 46.6. Overall, both PDF/FTC results and PDF/RFPV results are in good agreement with experimental data, which indicates that the present LES/PDF approach can capture the flow physics. While these results are encouraging, it has been noted in other studies [39] that even small errors in upstream results can lead to large errors in the prediction of soot further downstream.

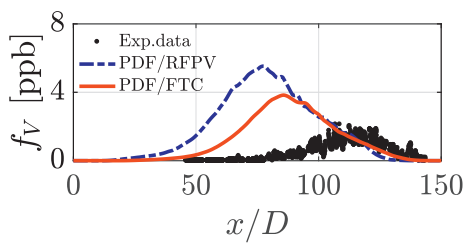


Fig. 3. Time-averaged soot volume fraction on the flame centerline.

In order to discuss the soot sensitivity to combustion model, Fig. 3 compares the LES/PDF results with experimental data for the soot volume fraction on the flame centerline. It is observed that both simulations capture soot volume fraction at downstream locations reasonably accurately, as compared to the presumed-PDF approach result [16]. In particular, the persistence of soot at locations downstream of $x/D = 120$ is captured well in this work. About 0.5-1 ppb soot can be observed in the PDF/RFPV model. However, the results from the presumed-PDF approach used in [16] seem to close to zero. Furthermore, both methods capture a lower peak soot volume fraction (about 5.5 ppb) than the presumed-PDF approach in [16] which predicted a peak soot volume fraction of about 7 ppb using the nominal constant for the subfilter dissipation rate model. In this sense, the use of the LES/PDF approach provides an improvement. Figure 3 shows that the location of soot inception predicted by the PDF/FTC model ($x/D \approx 50$) is more close to experimental measurement ($x/D \approx 70$) than that ($x/D \approx 30$) predicted by the PDF/RFPV model, which indicates the present PDF/FTC model has potential to reproduce the soot inception behavior. Moreover, the PDF/FTC model predicts a lower peak in soot volume fraction and a slightly shifted soot profiles towards the experimental data. This implies that soot growth processes, condensation and surface reaction, are significantly affected when accounting for the strong soot dependence on gas-phase composition through the PDF/FTC model. At $x/D > 100$, the decrease in soot volume fraction is caused by oxidation.

In order to determine the cause for reduction in centerline soot volume fraction with the

Please cite this article as: W. Han et al., Effects of combustion models on soot formation and evolution in turbulent nonpremixed flames, Proceedings of the Combustion Institute (2018), https://doi.org/10.1016/j.proci.2018.06.096

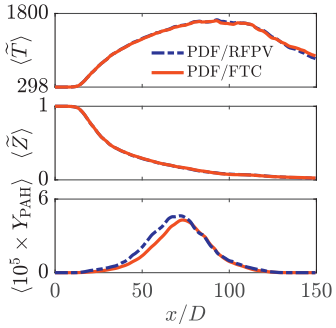


Fig. 4. Time-averaged temperature, mixture fraction, and PAH mass fraction on the flame centerline.

PDF/FTC model, the time-averaged temperature, mixture fraction, and PAH mass fraction on the flame centerline are shown in Fig. 4. It is observed that both the PDF/RFPV and PDF/FTC models predict the same mean profiles of temperature and mixture fraction along the flame centerline. The PDF/FTC model predicts slightly less PAH mass fraction than the PDF/RFPV model at upstream locations before $x/D = 80$, which can partly explain the less centerline soot volume fraction predicted by the PDF/FTC model.

### 5.3. Effects of combustion models on subfilter closure

To identify the underlying physical mechanisms captured with the PDF/FTC model, the effects of combustion models on the description of subfilter TCS interactions are investigated through the analysis of source terms of soot volume fraction. Figure 5 shows these source terms at four different axial locations ($x/D$ =65, 85, 110, and 125) covering the all phases of soot formation and evolution. It is observed that soot volume fraction source terms are considerably sensitive to combustion model. The PDF/FTC model predicts much lower soot mass addition through nucleation and condensation, especially at downstream locations. On the other hand, the PDF/FTC model shows increased surface growth using the HACA mechanism. It is found that soot oxidation is not sensitive to the TCS model. This is probably due to the fact that the oxidation rate coefficient that is tabulated in the chemistry table can be captured well

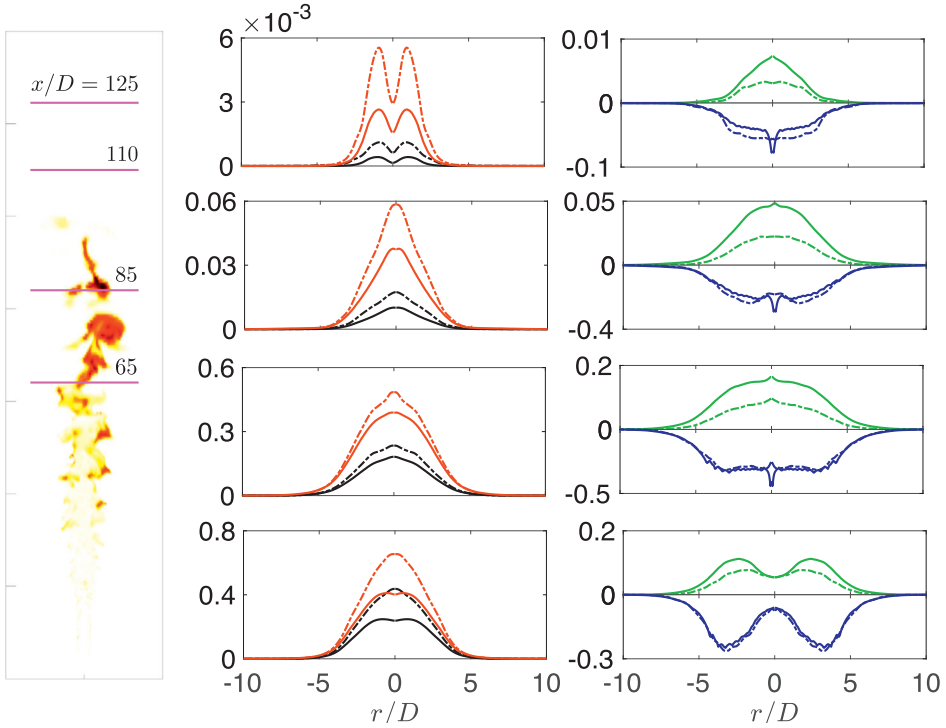


Fig. 5. Instantaneous of condensation (left) and radial profiles (middle and right) of the time-averaged soot volume fraction source terms [ppm/s]: nucleation (black lines), condensation (red lines), surface growth (green lines), and surface oxidation (blue lines) at four axial locations (from top to bottom) indicated in the left figure. Dash and solid lines correspond to LES/PDF/RFPV and LES/PDF/FTC, respectively. (For interpretation of the references to color in this figure legend, the reader is referred to the web version of this article.)

Please cite this article as: W. Han et al., Effects of combustion models on soot formation and evolution in turbulent nonpremixed flames, Proceedings of the Combustion Institute (2018), https://doi.org/10.1016/j.proci.2018.06.096

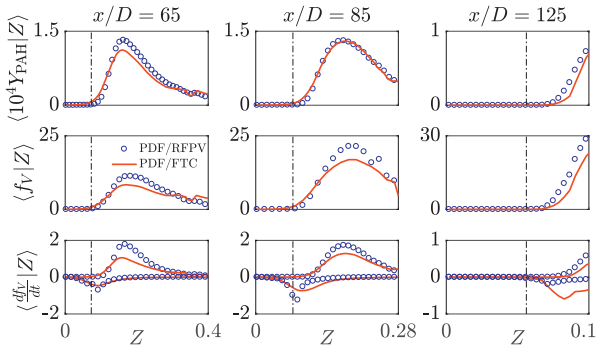


Fig. 6. Time-averaged conditional means of $Y_{\mathrm{PAH}}$, soot volume fraction [ppb], and soot volume fraction source terms [ppm/s]: nucleation+condensation (positive values), and surface oxidation (negative values). The stoichiometric mixture fraction is indicated by vertical dashed lines.

by the PDF/RFPV model. Furthermore, previous studies [3,16] concluded that the PAH-based soot growth mechanisms (nucleation and condensation) dominate over surface growth in turbulent jet flames. However, Fig. 5 shows that the contribution of surface growth is comparable in magnitude to the PAH-based growth, especially around the location of maximum volume fraction ($x/D = 85$). The reduced soot volume fraction along the centerline at upstream locations is essentially due to this reduction in nucleation and condensation processes. This indicates the choice of combustion model can significantly affect the description of subfilter TCS interactions.

In order to further study the sensitivity of subfilter TCS interactions to the combustion model, the conditional means of PAH mass fraction, soot volume fraction and its source terms are shown in Fig. 6. It is seen that soot volume fraction and soot growth through nucleation and condensation are maximum around the location of the highest PAH concentration ($Z = 0.15$) due to the strong correlation between soot dynamics and PAH. The two soot quantities slowly decline as the mixture becomes more rich. However, in leaner mixtures ($Z_{st} < Z < 0.15$), soot mass rapidly declines, which is due to the fact that the oxidation rates peak near the flame sheet with high temperature and the abundance of hydroxyl radical and molecular oxygen. Compared to the PDF/RFPV model, the PDF/FTC model suppresses/enhances soot growth/oxidation in mixture fraction space.

The above results indicate that the choice of combustion model has a significant impact on the description of soot formation and growth. This is due to the fact that turbulence, soot, and chemistry are tightly coupled at the sub-grid scales. In this sense, the PDF/RFPV model probably cannot capture the high sensitivity of soot formation and growth processes to the history of turbulent gas-phase compositions encountered. On the other hand, the PDF/FTC model has the potential to accurately describe detailed TCS interactions. As a result, the use of PDF/FTC model improves soot predictions. These findings highlight the importance of an accurate description of the strong TCS interactions in sooting turbulent flames.

## 6. Conclusions

In this work, a consistent LES/PDF approach has been further developed for modeling soot formation and evolution in turbulent nonpremixed flames with detailed chemistry. An accurate and efficient soot model based on the Hybrid Method of Moments (HMOM) was incorporated in the LES/PDF approach, considering detailed nucleation, condensation, coagulation, surface growth, oxidation, and fragmentation processes. To investigate the sensitivity of soot predictions to combustion model, the augmented LES/PDF approach was formulated with the FTC or RFPV combustion models. The Delft-Adelaide flame was simulated to understand the effects of combustion models on soot predictions. The following conclusions can be drawn based on this study:

- The PDF/FTC model accounting for detailed subfilter TCS interactions improves the simulation results and predicts lower soot volume fraction with soot formation and growth further downstream than the PDF/RFPV model. It is found that the location of inception and soot evolution are highly sensitive to the combustion model.
- In the context of LES, the choice of combustion model has a significant impact on the description of soot formation and growth. The decrease in the contributions of PAH-based soot growth (nucleation and condensation) is observed in the PDF/FTC model, while the contribution of acetylene-

Please cite this article as: W. Han et al., Effects of combustion models on soot formation and evolution in turbulent nonpremixed flames, Proceedings of the Combustion Institute (2018), https://doi.org/10.1016/j.proci.2018.06.096

based surface growth is enhanced and even dominates over condensation at downstream locations. Moreover, soot oxidation is not very sensitive to the choice of combustion model.
- The analyses of the source terms of soot volume fraction imply that the choice of combustion model can significantly affect the characterization of subfilter TCS interactions due to the strong coupling between turbulence, soot, and chemistry. The tabulated chemistry approach probably cannot capture the high sensitivity of soot formation and growth processes to the history of turbulent gas-phase compositions encountered. These findings indicate that the description of subfilter correlations between the gas-phase and the soot particles is of primary importance in affecting predictability.

While the cost of the PDF/FTC model is significantly higher and provides only comparable results to the PDF/RFPV model here, it is to be noted that the PDF/FTC model is more general and is valid in different combustion regimes. The current study is a first step in ensuring that the PDF/FTC model performs well in a regime that is specifically suited for flamelet-based models.

## Acknowledgments

VR and MEM gratefully acknowledge financial support from NASA through grant NNX16AP90A with Dr. Jeff Moder as program monitor. ZC would like to thank the support from National Natural Science Foundation of China (No. 91541204) and the High Performance Computing Platform at PKU.

## References

[1] N.H. Qamar, Z.T. Alwahabi, Q.N. Chan, G.J. Nathan, D. Roekaerts, K.D. King, *Combust. Flame* 156 (7) (2009) 1339–1347.
[2] K.P. Geigle, M. Köhler, W. O'Loughlin, W. Meier, *Proc. Combust. Inst.* 35 (2015) 3373–3380.
[3] F. Bisetti, G. Blanquart, M.E. Mueller, H. Pitsch, *Combust. Flame* 159 (2012) 317–335.
[4] H. Koo, M. Hassanaly, V. Raman, M.E Mueller, G.K. Peter, *ASME. J. Eng. Gas Turb. Power* 139 (3) (2016) 031503–031503–9.
[5] F. Bisetti, A. Attili, H. Pitsch, *Phil. Trans. R. Soc. A* 372 (2022) (2014) 20130324.
[6] V. Raman, R.O. Fox, *Annu. Rev. Fluid Mech.* 48 (2016) 159–190.
[7] M.E. Mueller, G. Blanquart, H. Pitsch, *Combust. Flame* 156 (2009) 1143–1155.
[8] I.M. Kennedy, *Prog. Energy Combust. Sci.* 23 (1997) 95–132.
[9] M. Frenklach, *Phys. Chem. Chem. Phys.* 4 (2002) 2028–2037.
[10] S.B. Pope, *Turbulent Flows*, Cambridge University Press, Cambridge, 2000.
[11] V. Raman, H. Pitsch, *Proc. Combust. Inst.* 31 (2007) 1711–1719.
[12] P. Donde, V. Raman, M.E. Mueller, H. Pitsch, *Proc. Combust. Inst.* 34 (1) (2013) 1183–1192.
[13] D.L. Marchisio, R.O. Fox, *Computational Models for Polydisperse Particulate and Multiphase Systems*, Cambridge University Press, Cambridge, 2013.
[14] R.O. Fox, *Computational Models for Turbulent Reacting Flows*, Cambridge University Press, Cambridge, 2003.
[15] R.O. Fox, *Annu. Rev. Fluid Mech.* 44 (2012) 47–76.
[16] M.E. Mueller, H. Pitsch, *Combust. Flame* 159 (2012) 2166–2180.
[17] Y. Xuan, G. Blanquart, *Proc. Combust. Inst.* 35 (2) (2015) 1911–1919.
[18] S. Deng, M.E. Mueller, Q.N. Chan, et al., *Proc. Combust. Inst.* 36 (1) (2017) 807–814.
[19] S.B. Pope, *Prog. Energy Combust. Sci.* 11 (1985) 119–192.
[20] W. Han, V. Raman, Z. Chen, *Combust. Flame* 171 (2016) 69–86.
[21] H. Wang, S.B. Pope, *Proc. Combust. Inst.* 33 (2011) 1319–1330.
[22] Z. Ren, S.B. Pope, *Proc. Combust. Inst.* 32 (2009) 1629–1637.
[23] F.A. Jaberi, P.J. Colucci, S. James, P. Givi, S.B. Pope, *J. Fluid Mech.* 401 (1999) 85–121.
[24] B. Zamuner, F. Dupoirieux, *Combust. Sci. Technol.* 158 (1) (2000) 407–438.
[25] R.S. Mehta, D.C. Haworth, M.F. Modest, *Combust. Flame* 157 (5) (2010) 982–994.
[26] R.P. Lindstedt, S.A. Louloudi, *Proc. Combust. Inst.* 30 (1) (2005) 775–783.
[27] F. Sewerin, S. Rigopoulos, *Phys. Fluids* 29 (2017) 105105.
[28] H. Wang, *Proc. Combust. Inst.* 33 (1) (2011) 41–67.
[29] K. Narayanaswamy, G. Blanquart, H. Pitsch, *Combust. Flame* 157 (10) (2010) 1879–1898.
[30] H. Wang, M. Frenklach, *Combust. Flame* 110 (1) (1997) 173–221.
[31] J. Villermaux, L. Falk, *Chem. Eng. Sci.* 49 (1994) 5127–5140.
[32] S.B. Pope, *J. Fluid Mech.* 652 (2010) 139–169.
[33] D.C. Haworth, *Prog. Energy Combust. Sci.* 36 (2010) 168–259.
[34] V. Raman, H. Pitsch, R.O. Fox, *Combust. Flame* 143 (2005) 56–78.
[35] S.B. Pope, *Combust. Theor. Model.* 1 (1997) 41–63.
[36] R.S. Barlow, A.N. Karpetis, J.H. Frank, J.Y. Chen, *Combust. Flame* 127 (3) (2001) 2102–2118.
[37] P.P. Popov, H. Wang, S.B. Pope, *J. Comput. Phys.* 294 (2015) 110–126.
[38] T. Peeters, P. Stroomer, J.E. de Vries, D. Roekaerts, C. Hoogendoorn, *Symp. (Int.) Combust.* 25 (1) (1994) 1241–1248.
[39] M.E. Mueller, V. Raman, *Combust. Flame* 161 (2014) 1842–1848.

Please cite this article as: W. Han et al., Effects of combustion models on soot formation and evolution in turbulent nonpremixed flames, Proceedings of the Combustion Institute (2018), https://doi.org/10.1016/j.proci.2018.06.096